methods

Identification of metabolites from Type III F_2-isoprostane diastereoisomers by mass spectrometry

Chiara Chiabrando,[1,*] Claudia Rivalta,[*] Renzo Bagnati,[*] Anna Valagussa,[*] Thierry Durand,[†] Alexandre Guy,[†] Pia Villa,[2,*] Jean-Claude Rossi,[†] and Roberto Fanelli[*]

Istituto di Ricerche Farmacologiche 'Mario Negri,'* Department of Environmental Health Sciences, Via Eritrea 62, 20157 Milano, Italy; and UMR CNRS 5074,† Faculty of Pharmacy, UM I, 15 Av. Ch. Flahault, F-34060 Montpellier, France

Abstract **F_2-isoprostanes (F_2-iPs) are prostaglandin (PG)-like products of non-enzymatic free radical-catalyzed peroxidation of arachidonic acid that are now widely used as indices of lipid peroxidation in vivo. Knowledge of the metabolic fate of F_2-iPs in vivo is still scant, despite its importance for defining their overall formation and biological effects in vivo. Type III F_2-iPs, which are diastereoisomers of cyclooxygenase-derived $PGF_{2\alpha}$, may be metabolized through the pathways of PG metabolism. We therefore studied the in vitro metabolism of eight synthetic Type III F_2-iP diastereoisomers in comparison with $PGF_{2\alpha}$. We used gas chromatography-mass spectrometry and high performance liquid chromatography-electrospray-tandem mass spectrometry for structural identification of metabolites formed after incubation of the various compounds with isolated rat hepatocytes. $PGF_{2\alpha}$ was metabolized to several known products, resulting from a combination of β-oxidation, reduction of Δ^5 and/or Δ^{13} double bonds, and 15-OH oxidation, plus other novel products deriving from conjugation with taurine of $PGF_{2\alpha}$ and its metabolites. Of the eight F_2-iP diastereoisomers, some were processed similarly to $PGF_{2\alpha}$, whereas others showed peculiar metabolic profiles according to specific stereochemical configurations. These data represent the first evidence of biodegradation of selected Type III F_2-iP isomers other than 8-*epi*-$PGF_{2\alpha}$, through known and novel pathways of $PGF_{2\alpha}$ metabolism. The analytical characterization of these products may serve as a basis for identifying the most significant products formed in vivo.**—Chiabrando, C., C. Rivalta, R. Bagnati, A. Valagussa, T. Durand, A. Guy, P. Villa, J-C. Rossi, and R. Fanelli. **Identification of metabolites from Type III F_2-isoprostane diastereoisomers by mass spectrometry. *J. Lipid Res.* 2002.** 43: **495–509.**

Supplementary key words $PGF_{2\alpha}$ • taurine conjugation • isolated rat hepatocytes • gas chromatography-mass spectrometry • high performance liquid chromatography-electrospray-tandem mass spectrometry

F_2-isoprostanes (F_2-iPs), a complex family of 64 compounds isomeric to cyclooxygenase-derived $PGF_{2\alpha}$, are products of non-enzymatic free radical-catalyzed peroxidation of arachidonic acid (1–3). Because these compounds are now widely used as indices of lipid peroxidation in vivo (2–5), knowledge of their metabolic fate may be useful, in general, to better define their overall formation. In fact, the identification of major metabolites of F_2-iPs might help in finding new analytical targets to monitor in addition to, or instead of, the parent compounds. Moreover, given that selected F_2-iP isomers have potent biological effects (2–5), it is important to establish whether and how these isomers are specifically degraded, to relate their levels in vivo to a putative biological effect.

Depending on the position of the free radical-initiated hydrogen abstraction, four classes of F_2-iP regioisomers can theoretically be formed by peroxidation of arachidonic acid. These families were first called Type I, II, III, and IV (1), but are now known as 5-, 12-, 8-, and 15-Series (2), or Type VI, V, IV, and III (6). Using the latter nomenclature (6), removal of a hydrogen at C-10 gives rise to the formation of two regioisomer families (Type IV and Type V), whereas at C-7 or C-13, it leads to the Type VI or Type III family, respectively. Regioisomer families of Type VI and Type III, theoretically predicted as the most abundant, did indeed predominate over Type V and IV in vivo (1, 6, 7).

F_2-iPs of Type III are of particular interest because they are diastereoisomers of cyclooxygenase-derived $PGF_{2\alpha}$ (**Fig. 1**), and may therefore mimic some of the biological properties of $PGF_{2\alpha}$ or other prostanoids. Although the biological effects of most F_2-iP isomers are largely unknown, 8-*epi*-$PGF_{2\alpha}$ and 12-*epi*-$PGF_{2\alpha}$ do indeed have biological effects that appear to be mediated

Abbreviations: GC, gas chromatography; iP, isoprostane; MO, methoxime; MS, mass spectrometry; MS/MS, tandem mass spectrometry; NICI, negative ion chemical ionization; PFB, pentafluorobenzyl ester; PG, prostaglandin; SIR, selected ion recording; SPE, solid phase extraction; TMS, trimethylsilyl ether.

[1] To whom correspondence should be addressed.
e-mail: chiabrando@marionegri.it
[2] Also affiliated with CNR, Cellular and Molecular Pharmacology Center, Via Vanvitelli, 32, 20129 Milano, Italy.

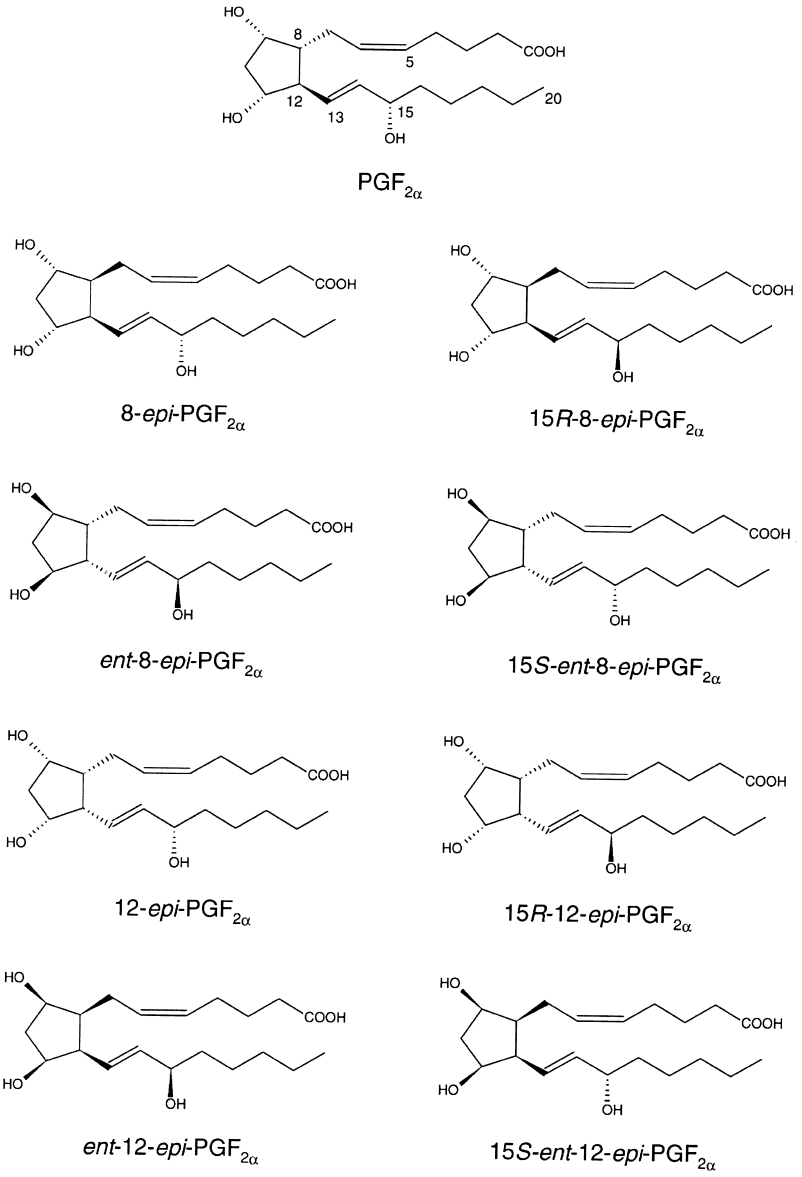

Fig. 1. Structures of $PGF_{2\alpha}$ and 8,12-*cis*-9,11-*cis* Type III F_2-iPs.

by prostanoid receptors (TP and/or FP) (2–5). In view of their structural similarity with $PGF_{2\alpha}$, Type III F_2-iPs may also interact with the enzymes that degrade prostaglandins in vivo, but it is difficult to predict the influence of the different steric configurations on the various metabolic pathways.

To date, the only F_2-iP metabolites identified as products of selected isomers are metabolites of 8-*epi*-$PGF_{2\alpha}$, the best-known and most-studied isomer (2–5). 2,3-Dinor-5,6-dihydro-8-*epi*-$PGF_{2\alpha}$ was reported as the only noteworthy metabolite of 8-*epi*-$PGF_{2\alpha}$ in humans (8). We have, however, recently shown that at least two major metabolites deriving from endogenous 8-*epi*-$PGF_{2\alpha}$ exist in human and rat urine (2,3-dinor-5,6-dihydro-8-*epi*-$PGF_{2\alpha}$ and 2,3-dinor-8-*epi*-$PGF_{2\alpha}$) (9). We also found that these same metabolites, in addition to 2,3,4,5-tetranor-8-*epi*-$PGF_{2\alpha}$, are formed when 8-*epi*-$PGF_{2\alpha}$ is incubated with isolated rat hepatocytes (9). In the rabbit, 13,14-dihydro-15-keto-2,3,4,5-tetranor-8-*epi*-$PGF_{2\alpha}$ was identified as the most abundant urinary metabolite of exogenous 8-*epi*-$PGF_{2\alpha}$ (10).

As we showed recently (9), searching for unknown endogenous metabolites of F_2-iPs is very complex, because of the simultaneous presence in vivo of a myriad of isomeric compounds. In fact, to obtain stereo- and enantio-specific identification of selected products, special analytical approaches have to be devised ad hoc (9). To obtain a general indication, as a first step, about which metabolites can be expected in vivo, we studied in vitro the metabolic fates of $PGF_{2\alpha}$ and Type III F_2-iPs. Among the 16 diastereoisomers of this family, we studied the eight with *cis* ring substituents, which are believed to be the most abundant (6) (Fig. 1). The different diastereoisomers were incubated with isolated rat hepatocytes, and their metabolites identified by gas chromatography-negative ion chemical ionization mass spectrometry (GC-NICIMS) and high-performance liquid chromatography-electrospray ionization-tandem mass spectrometry (HPLC-MS/MS).

MATERIALS AND METHODS

Materials

8-*Epi*-$PGF_{2\alpha}$, 3,3′,4,4′-[$^2H_4$]-8-*epi*-$PGF_{2\alpha}$, and 2,3-dinor-5,6-dihydro-8-*epi*-$PGF_{2\alpha}$ were purchased from Cayman Chemical Co. (Ann Arbor, MI). $PGF_{2\alpha}$ and 13,14-dihydro-15-keto-$PGF_{2\alpha}$ were from Upjohn Co. (Kalamazoo, MI). 15*R*-8-*epi*-$PGF_{2\alpha}$, *ent*-8-*epi*-$PGF_{2\alpha}$ (15*R* and 15*S*), 12-*epi*-$PGF_{2\alpha}$ (15*S* and 15*R*), *ent*-12-*epi*-$PGF_{2\alpha}$ (15*R* and 15*S*), 2,3-dinor-8-*epi*-$PGF_{2\alpha}$, 2,3-dinor-*ent*-8-*epi*-$PGF_{2\alpha}$, 2,3-dinor-5,6-dihydro-*ent*-8-*epi*-$PGF_{2\alpha}$, and 13,14-dihydro-15-keto-2, 3-dinor-5,6-dihydro-*ent*-8-*epi*-$PGF_{2\alpha}$ were synthesized in our laboratories (11–13).

Isolated rat hepatocytes

Hepatocytes were isolated as described previously (9) from fed male Crl:CD (SD) BR rats.[3] Briefly, hepatocytes obtained after perfusing the liver with a collagenase solution were washed and suspended in Leibovitz L-15 medium (Gibco, Scotland) supplemented with HEPES 18 mM, insulin (1 μg/ml), gentamicin (50 μg/ml), and 5% FCS (Gibco) at a density of 1×10^6 cells/ml. After 3 h adhesion the medium was replaced, but without FCS and gentamicin.

Incubation of $PGF_{2\alpha}$ and related F_2-iPs

Plates were prepared with 3×10^6 cells. The incubation medium was enriched with 670 ng/ml of $PGF_{2\alpha}$, 8-*epi*-$PGF_{2\alpha}$, or the other F_2-iPs under test. In a preliminary experiment to test the experimental conditions, cells were incubated for 10, 20, and 40 min with or without $PGF_{2\alpha}$ and 8-*epi*-$PGF_{2\alpha}$. In the other experiments, $PGF_{2\alpha}$ and the various F_2-iPs were incubated separately for 20 min. At the end of the incubation, the medium was collected and spun at 4°C to eliminate non-adhering hepatocytes. Cell-free medium ad plates were stored at −20°C until analyzed.

Extraction

Metabolites were extracted from the incubation medium (2.5 ml) after addition of [$^2H_4$]-8-*epi*-$PGF_{2\alpha}$ and [$^2H_4$]-$PGF_{2\alpha}$ (50 ng each) as internal standards. The medium was diluted to 10 ml with 1 mM HCl, acidified to pH 3, and extracted on C18 solid phase extraction columns (SPE; Bakerbond) preconditioned with methanol and 1 mM HCl. After two washing steps (water and petroleum ether, 10 ml each), the columns were eluted with 2 ml methyl formate (eluate A) and then 2 ml methanol (eluate B). After drying, eluates were assayed separately as follows. Eluate A (containing the unmetabolized parent compounds and unconjugated metabolites), was derivatized (see below) and analyzed by GC-NICIMS, or reconstituted in the HPLC initial mobile phase (see below) and directly analyzed by HPLC-MS/MS. Eluate B (containing conjugated metabolites), was analyzed by HPLC-MS/MS. Metabolites were also extracted from plate-adhering hepatocytes by *1*) adding ethanol and internal standards to plates (4°C overnight), *2*) suspending the cell lysate, *3*) vigorously vortexing, centrifuging and drying the ethanol suspension, and *4*) resuspending the residue in 1 mM HCl and extracting as above. In experiments to measure the unmetabolized parent compounds, 0.025 ml medium and 5 ng internal standards were used.

[3] Procedures involving animals and their care were conducted in conformity with the institutional guidelines that are in compliance with national (D.L. n. 116, G.U., suppl. 40, 18 Febbraio 1992, Circolare No. 8, G.U., 14 Luglio 1994) and international laws and policies (EEC Council Directives 86/609, OJ L 358, 1, Dec. 12, 1987; Guide for the Care and Use for Laboratory Animals, U.S. National Research Council, 1996).

Derivatization

Samples were converted to pentafluorobenzyl ester (PFB), methoxime (MO), and trimethylsilyl ethers (TMS), or PFB-TMS as follows: *1*) add 30 μl pentaflourobenzyl bromide-acetonitrile (1:5, v/v) and 5 μl diisopropylethylamine to the dry residue (40°C for 5 min); *2*) repeat previous step; *3*) add 50 μl methoxyamine HCl in pyridine (Pierce, Rockford, IL), (60°C for 1 h); *4*) dry; and *5*) add 50 μl *N,O-bis*-(trimethylsilyl)trifluoroacetamide (Fluka, Buchs, Switzerland) (60°C for 1 h).

GC-NICIMS

Analyses were as described (9), using a Finnigan 4000 mass spectrometer. Briefly, GC operating conditions were: NB-54 (5% phenyl, 95% dimethylpolysiloxane) fused silica capillary column (25 m length, 0.32 mm ID, 0.12 μm film thickness); solvent-split injection (50°C to 300°C); oven temperature, isothermal at 160°C for 1 min, then programmed to 300°C at 10°/min; helium as carrier gas. Negative ion chemical ionization (NICI) operating conditions were: selected ion recording (SIR) of carboxylate anions (M-181, loss of PFB); methane as reagent gas; electron energy, 100 eV.

HPLC-MS/MS

Analyses were done on an API 3000 triple quadrupole instrument (PE Sciex, Thornhill, Ontario, Canada), interfaced with two Series 200 micro liquid chromatography (LC) pumps (Perkin-Elmer, Norwalk, CT). HPLC conditions were as follows: column, Superspher C_{18e}, 3.5 μm, 2 × 125 mm (Merck, Darmstadt, Germany); flow, 0.2 ml/min; eluent A, 0.1% formic acid; eluent B, acetonitrile; gradient, from 10% to 52% B in 28 min; loop, 20 μl. The HPLC effluent was directed to the MS instrument through a splitting T-connection, reducing the flow into the ion source to about 40 μl/min. MS conditions were as follows: source, Turbo-IonSpray in negative ion mode; heater gas, 280°C; ion spray voltage, −4,000 V; orifice voltage, −56 V; ring voltage, −250 V; collision cell gas, nitrogen at a pressure of 2.6×10^{-5} torr; collision energy, 26 to 56 eV (see Results). To optimize ionization and Q2 decomposition, authentic standards were directly infused into the ion source, or MS/MS loop experiments with different collision energies were run on the HPLC-eluted biological material.

Metabolite quantitation

To compare the metabolic profiles of unconjugated metabolites of the various diastereoisomers, we assayed the hepatocyte medium by GC-NICIMS in the SIR mode. In these experiments, $^2H_4$-8-*epi*-$PGF_{2\alpha}$ (5 ng) was added to 0.25 ml of incubation medium before C18 solid phase extraction (SPE). Quantitation was done by comparing peak area ratios of the carboxylate anion of each metabolite to that of the internal standard, using for reference the calibration curve of 8-*epi*-$PGF_{2\alpha}$/$^2H_4$-8-*epi*-$PGF_{2\alpha}$ (9). This was done assuming that all metabolites gave an approximately similar molar response on the NICIMS recording of their respective carboxylate anions (9). For compounds bearing the 15-keto group, giving syn/anti isomers of the methoxime derivative, the total peak area was used for calculation.

RESULTS

Identification strategy for $PGF_{2\alpha}$ and F_2-iPs

The hepatocyte incubation medium was first screened for the presence of major metabolites of $PGF_{2\alpha}$ and 8-*epi*-$PGF_{2\alpha}$ by GC-NICIMS. We based ourselves on earlier descriptions of $PGF_{2\alpha}$ metabolism in various species (14–19)

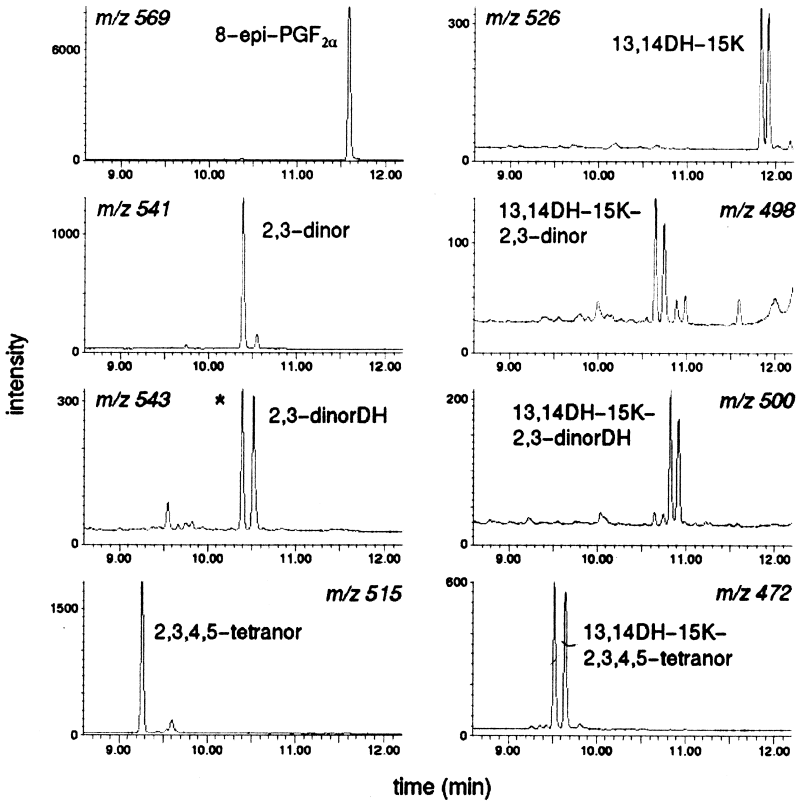

Fig. 2. Gas chromatography-negative ion chemical ionization mass spectrometry (GC-NICIMS) selected ion recording tracing of carboxylate anions $(M\text{-}PFB)^-$ of 8-*epi*-$PGF_{2\alpha}$ and its unconjugated metabolites formed by isolated rat hepatocytes. The compounds were extracted from the incubation medium and derivatized to pentafluorobenzyl ester/methoxime/trimethylsilyl ether (PFB/MO/TMS). 13,14DH-15K, 13,14-dihydro-15-keto; 2,3-dinorDH, 2,3-dinor-5,6-dihydro. The peak labeled with an asterisk is from the isotopic cluster of 2,3-dinor metabolite.

and our previous characterization of β-oxidation products of $PGF_{2\alpha}$ and 8-*epi*-$PGF_{2\alpha}$ (9), and used full scan and SIR to screen for the carboxylate anion clusters of the PFB esters of metabolites possibly formed from the nine diastereoisomers. **Figure 2** shows a representative SIR tracing of the unconjugated metabolites of 8-*epi*-$PGF_{2\alpha}$.

The unconjugated products tentatively identified by this screening method were then structurally identified after HPLC separation by examining the mass spectra of the product ions formed after collision-activated decomposition (CAD) of the carboxylate anions produced by electrospray ionization (HPLC-MS/MS) (**Table 1**). **Figure 3** shows a representative HPLC-MS/MS tracing of the unconjugated metabolites of 8-*epi*-$PGF_{2\alpha}$.

Chromatographic and mass spectral features of parent compounds, their metabolites, and authentic standards are summarized in **Table 2** (GC-NICIMS) and **Table 3** (HPLC-MS/MS). $PGF_{2\alpha}$ and its two epimers at C-8 (8-*epi*-$PGF_{2\alpha}$) and C-12 (12-*epi*-$PGF_{2\alpha}$) gave excellent separation by both GC and HPLC, and their corresponding epimeric

TABLE 1. Metabolites of $PGF_{2\alpha}$ and F_2-iPs identified[a] in isolated rat hepatocyte incubation media

Modifications of PGF_2 Structure	$PGF_{2\alpha}$	8-*epi*	*ent*-8-*epi*	15*R*-8-*epi*	15*S*-*ent*-8-*epi*	12-*epi*	*ent*-12-*epi*	15*R*-12-*epi*	15*S*-*ent*-12-*epi*
C20									
1-Tauro	+	+	+	+	+	+	+	+	+
13,14DH-15K	+	+			+				
1-Tauro-13,14DH-15K	+	+			+				
C18									
2,3-Dinor		+	+	+	+	+	+		
1-Tauro-2,3-dinor		+		+		+	+		
13,14DH-15K-2,3-dinor		+							
1-Tauro-13,14DH-15K-2,3-dinor		+							
C18									
2,3-dinorDH	+	+	+			+	+		
1-Tauro-2,3-dinorDH	+					+	+		
13,14DH-15K-2,3-dinorDH	+	+							
1-Tauro-13,14DH-15K-2,3dinorDH	+								
C16									
2,3,4,5-Tetranor	+	+	+	+	+	+	+	+	+
13,14DH-15K-2,3,4,5-tetranor	+	+	+		+	+	+		

1-Tauro, taurine conjugate at C-1; 13,14DH-15K, 13,14-dihydro-15-keto; 2,3-dinorDH, 2,3-dinor-5,6-dihydro.
[a] Unconjugated metabolites were identified by both GC-NICIMS and HPLC-MS/MS, and taurine conjugates by HPLC-MS/MS.

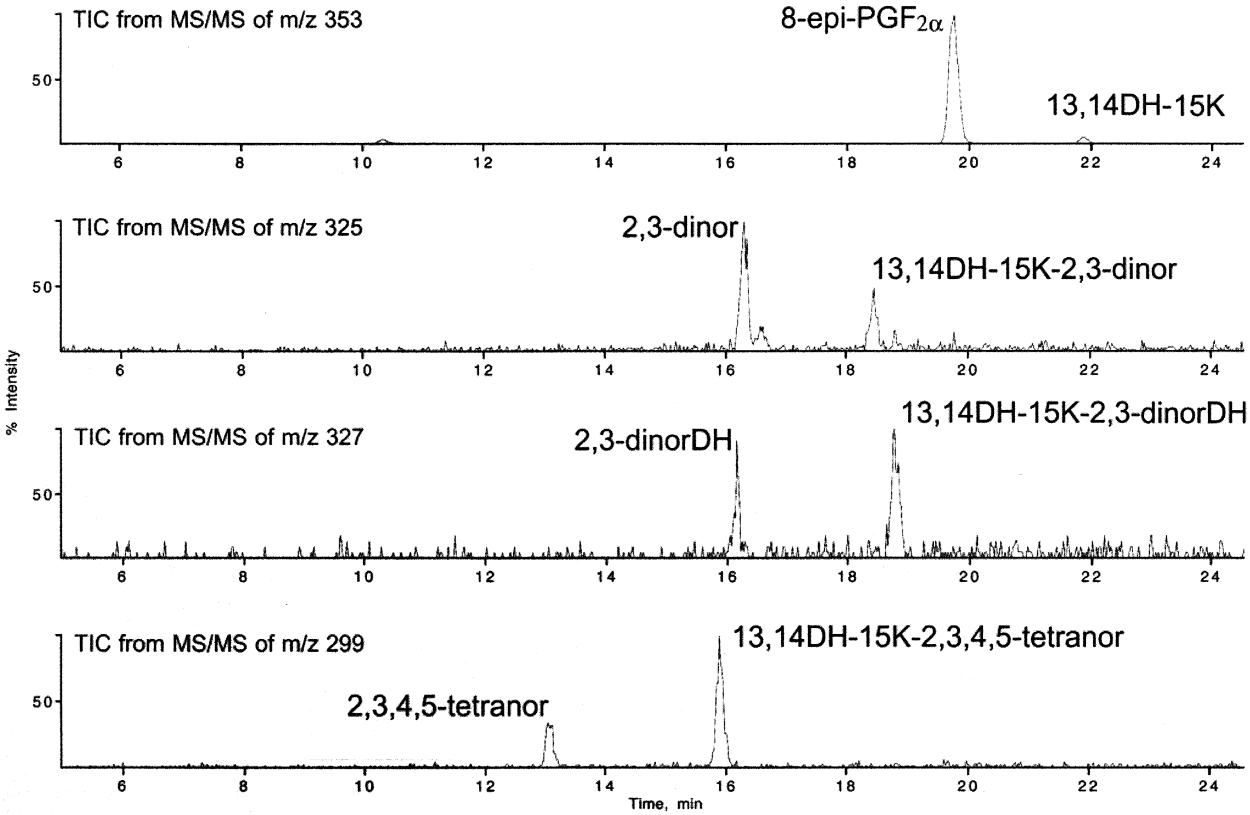

Fig. 3. High-performance liquid chromatography-tandem mass spectrometry (HPLC-MS/MS) tracing of total ion current (TIC) of product ions generated by collision-activated decomposition of carboxylate anions $(M\text{-}H)^-$ of 8-*epi*-$PGF_{2\alpha}$ and its unconjugated metabolites formed by isolated rat hepatocytes. The compounds were extracted from the incubation medium. 13,14DH-15K, 13,14-dihydro-15-keto; 2,3-dinorDH, 2,3-dinor-5,6-dihydro.

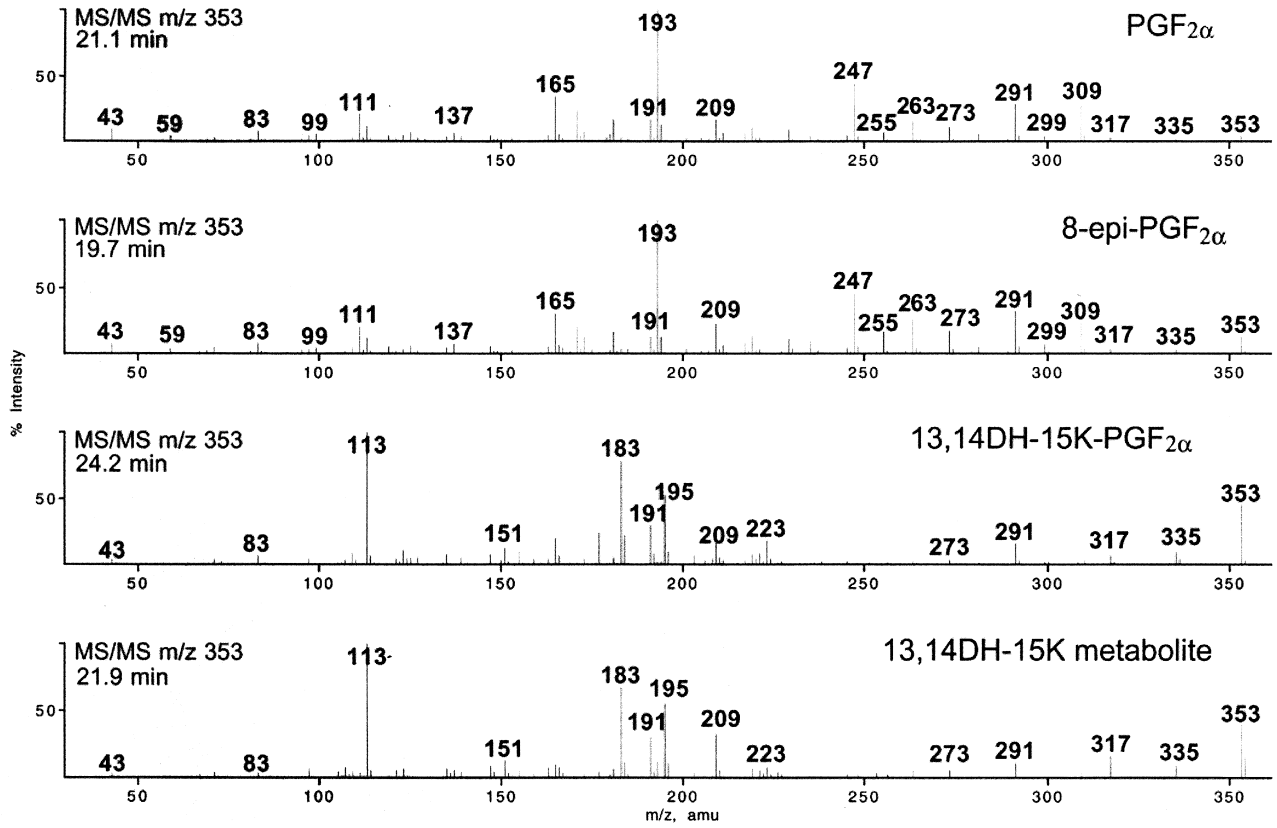

Fig. 4. Tandem mass spectrometry (MS/MS) spectra obtained from collision-activated decomposition of the carboxylate anions (*m/z* 353; 38 eV) of parent $PGF_{2\alpha}$ and 8-*epi*-$PGF_{2\alpha}$, plus authentic 13,14-dihydro-15-keto-$PGF_{2\alpha}$ and hepatocyte-derived 13,14-dihydro-15-keto-8-*epi*-$PGF_{2\alpha}$. HPLC retention time is indicated for each metabolite.

TABLE 2. GC-NICIMS behavior of $PGF_{2\alpha}$, Class III F_2-iPs and their unconjugated metabolites as PFB-TMS or PFB-MO-TMS[a] derivatives

Modifications of PGF_2 Structure	[M-PFB]$^-$	GC Retention Time								
		$PGF_{2\alpha}$	8-*epi*	*ent*-8-*epi*	15*R*-8-*epi*	15*S*-*ent*-8*epi*	12-*epi*	*ent*-12-*epi*	15*R*-12-*epi*	15*S*-*ent*-12*epi*
	m/z					*min*				
Parent PGF_2 compounds ($PGF_{2\alpha}$ or F_2-iP)	569	11.9	11.6	11.6	11.5	11.5	11.8	11.8	11.8	11.8
13,14DH-15K metabolites	526	12.0	11.8/11.9			11.7/11.8				
Standard: 13,14DH-15K- $PGF_{2\alpha}$	526	12.0								
2,3-Dinor metabolites	541		10.4	10.4	10.4		10.6	10.6		
Standard: *ent*-2,3-dinor-8-*epi*-$PGF_{2\alpha}$	541			10.4						
13,14DH-15K-2,3-dinor metabolites	498		10.7/10.8							
2,3-Dinor-5,6DH metabolites	543	10.8	10.5	10.5			10.8	10.8		
Standard: 2,3-dinor-5,6-dihydro-8-*epi*-PGF_{2a}	543		10.5							
13,14DH-15K-2,3-dinor-5,6DH metabolites	500	11.0	10.8/10.9							
Standard: 13,14DH-15K-2,3-dinor-5,6DH-*ent*-8-*epi*-PGF_{2a}	500			10.8/10.9						
2,3,4,5-Tetranor metabolites	515	9.5	9.2	9.2	9.2	9.2	9.4	9.4	9.4	9.4
13,14DH-15K-2,3,4,5-tetranor metabolites	472	9.6	9.5/9.6	9.5/9.6		9.5/9.6	9.6	9.6		

13,14DH-15K, 13,14-dihydro-15-keto; 5,6DH, 5,6-dihydro.

[a] Peak doublets for MO derivatives of 15K compounds are due to syn/anti isomers.

TABLE 3. HPLC-MS/MS behavior of $PGF_{2\alpha}$, Class III F_2-iPs and their unconjugated metabolites

Modifications of PGF_2 Structure	[M-H]$^-$	HPLC Retention Time								
		$PGF_{2\alpha}$	8-*epi*	*ent*-8-*epi*	15*R*-8-*epi*	15*S*-*ent*-8-*epi*	12-*epi*	*ent*-12-*epi*	15*R*-12-*epi*	15*S*-*ent*-12-*epi*
	m/z					*min*				
Parent PGF_2 compounds ($PGF_{2\alpha}$ or F_2-iP)	353	21.1	19.7	19.7	19.7	19.7	20.7	20.7	21.5	21.5
13,14DH-15K metabolites	353	24.2	21.9			21.9				
Standard: 13,14DH-15K-$PGF_{2\alpha}$	353	24.2								
2,3-Dinor metabolites	325		16.3	16.3	16.4		17.1	17.1		
Standard: 2,3-dinor-*ent*-8-*epi*-$PGF_{2\alpha}$	325			16.3						
13,14DH-15K-2,3-dinor metabolites	325		18.9							
2,3-Dinor-5,6DH metabolites	327	17.5	16.2	16.2			16.5	16.5		
Standard: 2,3-dinor-5,6-dihydro-8-*epi*-$PGF_{2\alpha}$	327		16.2							
13,14DH-15K-2,3-dinor-5,6DH metabolites	327	21.0	18.7							
Standard: 2,3-dinor-5,6-dihydro-13,14DH-15K-*ent*-8-*epi*-$PGF_{2\alpha}$	327			18.7						
2,3,4,5-Tetranor metabolites	299	14.4	13.2	13.2	13.9	13.9	12.9	12.9	(13.8)	(13.8)
13,14DH-15K-2,3,4,5-tetranor metabolites	299	17.5	15.9	15.9		16.0	18.5	18.5		

13,14DH-15K, 13,14-dihydro-15-keto; 5,6DH, 5,6-dihydro.

metabolites behaved similarly (Tables 2 and 3). For all compounds, the steric configuration of the hydroxyl at C-15 had little or no influence on the retention time in both techniques in the conditions used (Tables 2 and 3). The enantiomeric pairs (e.g., 8-*epi*-$PGF_{2\alpha}$ and *ent*-8-*epi*-$PGF_{2\alpha}$) showed the expected identical behavior, since they obviously need a chiral separation step to be resolved (Tables 2 and 3). All diastereoisomers gave identical MS/MS spectra, as shown for example for $PGF_{2\alpha}$ and 8-*epi*-$PGF_{2\alpha}$ (**Fig. 4**), as reported by Waugh et al. (7).

Most unconjugated compounds were identified by direct comparison with the corresponding standard synthesized ad hoc in our laboratories (Tables 2, 3, and **Table 4**). Metabolites lacking the corresponding reference compounds were identified by comparison with an authentic diastereoisomeric analog (Tables 2 and 3). Additional identification criteria are described below in the specific sections. MS/MS spectra of selected diastereoisomeric unconjugated metabolites are shown in Fig. 4, **Figs. 5** and **6**.

For simplicity, the various diastereoisomeric metabolites identified for $PGF_{2\alpha}$ and F_2-iPs are described by referring to their common chemical structure. Identification criteria for conjugated metabolites are reported below.

Metabolites of $PGF_{2\alpha}$ and Type III F_2-iPs

Metabolism of $PGF_{2\alpha}$ by isolated rat hepatocytes was studied as a reference for the eight 8,12-*cis*-9,11-*cis* Type III F_2-iP diastereoisomers (Fig. 1). Some of the compounds identified here as $PGF_{2\alpha}$ metabolites are products of known metabolic pathways, i.e., one or two steps of β-oxidation, reduction of Δ^5 and/or Δ^{13} double bonds, and 15-OH dehydrogenation (**Fig. 7**). We also identified novel taurine conjugates of $PGF_{2\alpha}$ and its metabolites. Some, but not all, of these compounds were also formed from F_2-iPs, which were in fact metabolized according to stereoselective patterns (Table 1).

The overall view of the metabolites identified for the nine PGF_2 diastereoisomers (Table 1) shows that: *1*) all metabolites of $PGF_{2\alpha}$ were also present as products of some, although not all, F_2-iPs; *2*) some metabolites were exclusive products of F_2-iPs (i.e., all 2,3-dinor metabolites with intact Δ^5 double bond); *3*) among F_2-iPs, 8-*epi*-$PGF_{2\alpha}$ had the largest number of products in common with $PGF_{2\alpha}$; *4*) the only products common to all nine diastereoisomers were the 2,3,4,5-tetranor metabolites and the taurine conjugates of the parent compounds; *5*) within the 8-*epi* series, those with the 15*R* configuration were not transformed into any of the seven possible metabolites bearing the 13,14-dihydro-15-keto modification; and *6*) within the 12-*epi* series, each enantiomeric pair showed a characteristic profile.

Unconjugated metabolites. To help interpret the MS/MS spectra of the metabolites, the product ions formed from the precursor carboxylate anions of the metabolites are listed in Table 4 in comparison with those of parent $PGF_{2\alpha}$ or F_2-iPs, plus 3,3′,4,4′-$^2H_4$-8-*epi*-$PGF_{2\alpha}$, and 1,1′-$^{18}O_2$-2,3-dinor-5,6-dihydro-8-*epi*- $PGF_{2\alpha}$. All mass spectral data refer to authentic standards and corresponding metabolites, except for hepatocyte-derived 13,14-dihydro-15-keto-2,3-dinor metabolite and the two tetranor compounds. The structural interpretation given in Table 4 is mainly based on work by Murphy's group (7, 20–21), or deducted from the comparison of the various metabolites and stable isotope-labeled analogs. Product ions of the carboxylate anion of 8-*epi*-$PGF_{2\alpha}$ or $PGF_{2\alpha}$, that reportedly comprise the α-chain, had the expected counterparts in the α-chain shortened metabolites, with shifts of 28 amu less (2,3-dinor), 26 amu less (2,3-dinor-5,6-dihydro), and 54 amu less (2,3,4,5-tetranor) (Table 4). This and other specific features described below allowed identification of the three compounds for which no authentic standard was available.

2,3-DINOR METABOLITE. No compound with a 2,3-dinor modification and intact Δ^5 double bond was found for $PGF_{2\alpha}$, confirming previous observations in the rat in vitro and/or in vivo by ourselves (9) and others (16–18). The 2,3-dinor metabolite was, however, identified as a prominent product of several F_2-iP diastereoisomers, namely 8-*epi*-$PGF_{2\alpha}$, 15*R*-8-*epi*-$PGF_{2\alpha}$, *ent*-8-*epi*-$PGF_{2\alpha}$, 15*S*-*ent*-8-*epi*-$PGF_{2\alpha}$, 12-*epi*-$PGF_{2\alpha}$, and *ent*-12-*epi*-$PGF_{2\alpha}$ (Tables 1, 2, 3). 2,3-Dinor-8-*epi*-$PGF_{2\alpha}$, which we had characterized previously as a prominent endogenous metabolite in human and rat urine, as well as a major product of 8-*epi*-$PGF_{2\alpha}$ metabolism by rat hepatocytes, was now compared with authentic 2,3-dinor-8-*epi*-$PGF_{2\alpha}$ recently synthesized in our laboratories (Fig. 5). While the carboxylate anions of parent compounds and other metabolites produced several fragment ions mainly due to single and combined losses of H_2O, CO_2, and C_2H_4O from the ring, and various parts of the alkyl chains (7, 20–21), the carboxylate anion of the 2,3-dinor metabolite (*m/z* 325) gave a peculiar fragmentation (Table 4 and Fig. 5). Even at a low collision energy (22 eV), its MS/MS spectrum was dominated by a main fragment ion at *m/z* 237, probably due to the loss of C_2H_4O plus CO_2 from the carboxyl. Other minor ions were observed at *m/z* 263 (loss of H_2O and C_2H_4O), *m/z* 219 (loss of H_2O, C_2H_4O and CO_2), *m/z* 163 (loss of H_2O, CO_2 and hexanal), and *m/z* 137. Similar MS/MS spectra (not shown) were recorded for the corresponding metabolites derived from the other F_2-iPs.

2,3-DINOR-5,6-DIHYDRO METABOLITE. This was a prominent product of $PGF_{2\alpha}$, 12-*epi*-$PGF_{2\alpha}$, and *ent*-12-*epi*-$PGF_{2\alpha}$, and a minor product of 8-*epi*-$PGF_{2\alpha}$ and *ent*-8-*epi*-$PGF_{2\alpha}$ (Tables 1–3). These compounds were identified by direct comparison with commercial 2,3-dinor-5,6-dihydro-8-*epi*-$PGF_{2\alpha}$ and synthetic 2,3-dinor-5,6-dihydro-*ent*-8-*epi*-$PGF_{2\alpha}$. Figure 6 shows the MS/MS spectra of authentic 2,3-dinor-5,6-dihydro-8-*epi*-$PGF_{2\alpha}$ and hepatocyte-derived 2,3-dinor-5,6-dihydro-$PGF_{2\alpha}$, as an example. The precursor ion (*m/z* 327) was fragmented according to the typical pattern of the PGF_2 compounds (Table 4). The MS/MS spectrum of 2,3-dinor-5,6-dihydro-8-*epi*-$PGF_{2\alpha}$ labeled with $^{18}O_2$ enabled us to confirm the proposed fragmentation by observing the expected shift of 4 amu in all fragment ions conserving the carboxyl (Table 4). However, the ion at *m/z* 167 did not shift to *m/z* 171, as expected, when the carboxyl was labeled with $^{18}O_2$. The putatively corresponding ion of 8-*epi*-$PGF_{2\alpha}$ at *m/z* 193 shifts in fact to *m/z* 197 upon label-

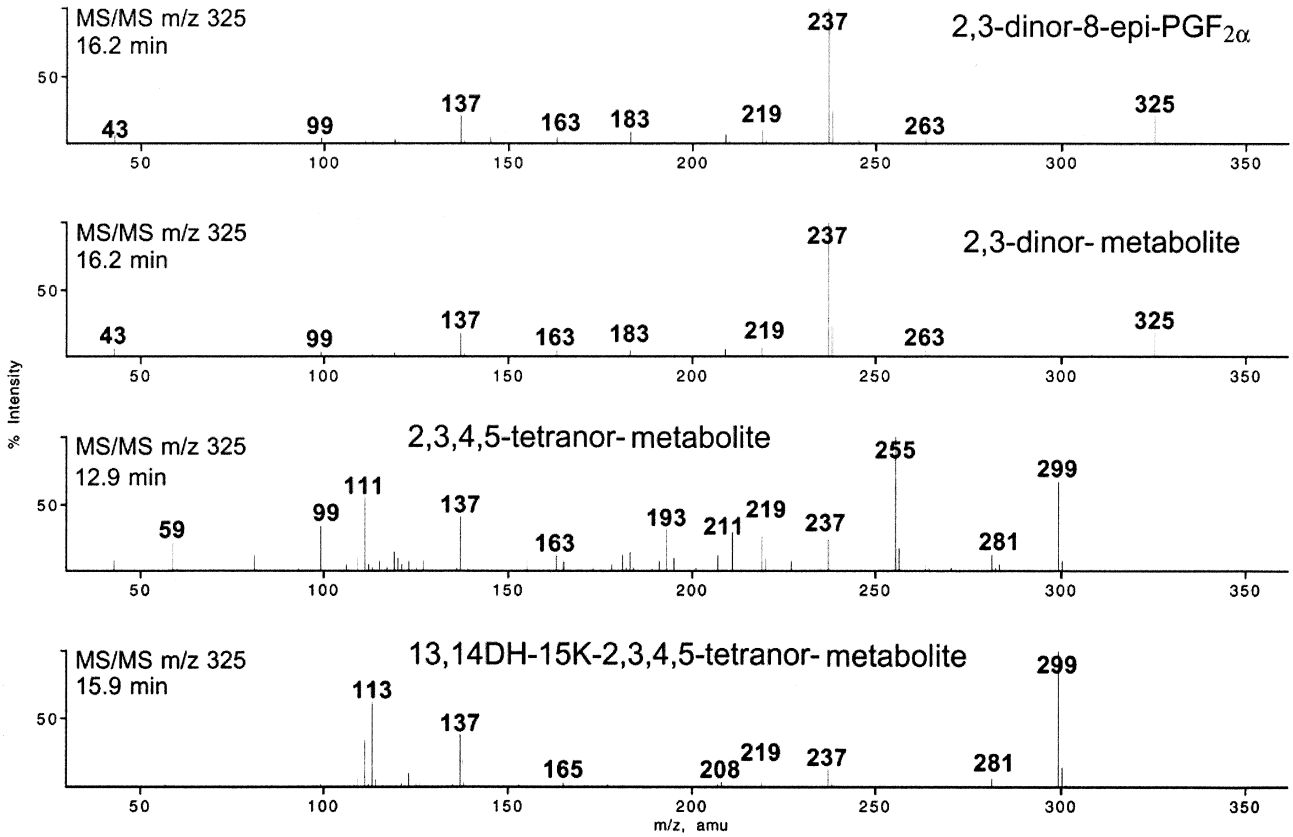

Fig. 5. MS/MS spectra obtained from collision-activated decomposition of the carboxylate anions of authentic 2,3-dinor-8-*epi*-$PGF_{2\alpha}$ and hepatocyte-derived 2,3-dinor-8-*epi*-$PGF_{2\alpha}$ (*m/z* 325; 22 eV), and hepatocyte-derived 2,3,4,5-tetranor-8-*epi*-$PGF_{2\alpha}$ and 13,14-dihydro-15-keto-2,3,4,5-tetranor-8-*epi*-$PGF_{2\alpha}$ (*m/z* 299; 30 eV). HPLC retention time is indicated for each metabolite.

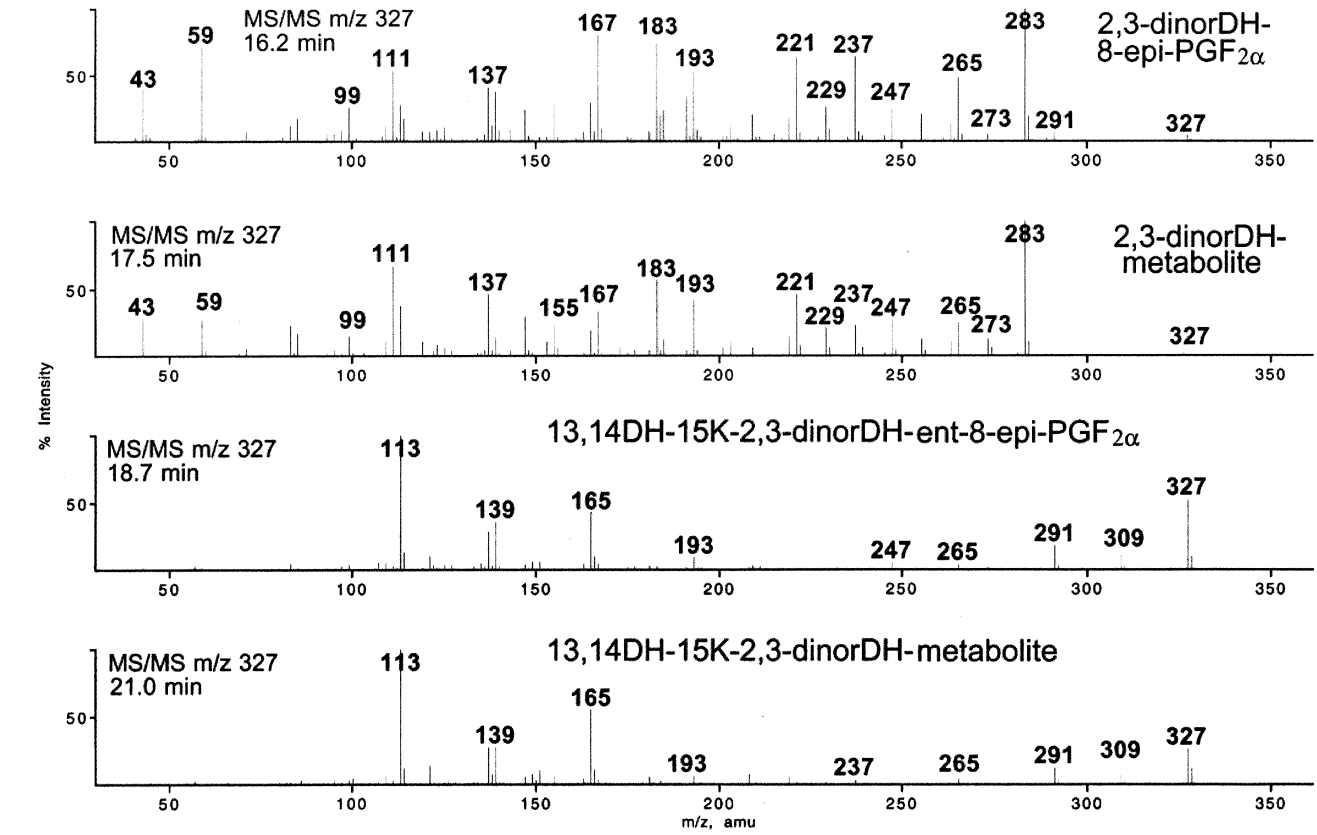

Fig. 6. MS/MS spectra obtained from collision-activated decomposition of the carboxylate anions (*m/z* 327; 40 eV) of authentic 2,3-dinor-5,6-dihydro-8-*epi*-$PGF_{2\alpha}$, hepatocyte-derived 2,3-dinor-5,6-dihydro-$PGF_{2\alpha}$, authentic 13,14-dihydro-15-keto-2,3-dinor-5,6-dihydro-*ent*-8-*epi*-$PGF_{2\alpha}$, and hepatocyte-derived 13,14-dihydro-15-keto-2,3-dinor-5,6-dihydro-$PGF_{2\alpha}$. HPLC retention time is indicated for each metabolite.

TABLE 4. Product ions[a] detected by MS/MS after fragmentation of carboxylate anions [M-H]$^-$ of $PGF_{2\alpha}$, Class III F_2-iPs and their unconjugated metabolites

Modifications of PGF_2 Structure	Compound[b]	[M-H]$^-$	-H_2O	-2(H_2O)	-C_2H_4O	-3(H_2O)	-H_2O -C_2H_4O	-2(H_2O) -(CO_2 or C_2H_4O)	-C_2H_4O -CO_2	-H_2O -(C16 -C20)	-3(H_2O) -CO_2	-H_2O -C_2H_4O -CO_2	-C_2H_4O -hexanal	-C_2H_4O -(C14 -C20)	-C_2H_4O -CO_2 -(C16-C20)	-H_2O -hexanal -CO_2
		m/z														
$PGF_{2\alpha}$ or Class III F_2-iP	St	353	335	317	309	299	291	273		263	255	247	209	193		191
3,3′,4,4′-$^2H_4PGF_{2\alpha}$	St	357	339	321	313	303	295	277		267	259	251	213	197		195
13,14DH-15K	St; M	353	335	317			291	273					209			191
2,3-dinor	St; M	325					263	245	237			219				163
13,14DH-15K-2,3-dinor	M	325					263	245								163
2,3-dinor-5,6DH	St; M	327	309	291	283	273	265	247		237	229	221	183		167	165
1,1′-$^{18}O_2$-2,3-dinor-5,6DH	St	331	313	295	287		269	247		241	229	221	187		167	165
13,14DH-15K-2,3-dinor-5,6DH	St; M	327	309	291			265	247								165
2,3,4,5-tetranor	M	299	281		255		237	219	211		201	193				137
13,14DH-15K-2,3,4,5-tetranor	M	299	281				237	219								137

[a] For other product ions lacking obvious interpretation, see Figs. 4–6.
[b] Data from: Standard (St) and/or hepatocyte-derived metabolite (M).

TABLE 5. HPLC-MS/MS behavior of taurine conjugates of $PGF_{2\alpha}$, Class III F_2-iPs and their metabolites

Modifications of PGF_2 Structure	[M-H]$^-$	HPLC Retention Time								
		$PGF_{2\alpha}$	8-*epi*	*ent*-8-*epi*	15*R* 8-*epi*	*ent*-8-*epi*-15*S*	12-*epi*	*ent*-12-*epi*	15*R*-12-*epi*	15S-*ent*-12-*epi*
	m/z					*min*				
1-Tauro	460	13.3	12.4	12.1	12.4	12.1	12.5	12.5	12.7	12.7
1-Tauro 13,14DH-15K	460	14.6	13.3	—	—	13.3	—	—	—	—
1-Tauro 2,3-dinor	432	—	9.1	—	—	—	—	—	—	—
1-Tauro-13,14DH-15K-2,3-dinor	432	—	10.5	—	—	—	—	—	—	—
1-Tauro-2,3-dinor-5,6DH	434	10.4	—	—	—	—	—	—	—	—
1-Tauro-13,14DH-15K-2,3-dinor-5,6DH	434	12.3	—	—	—	—	—	—	—	—

1-Tauro, taurine conjugate at C-1; 13,14DH-15K, 13,14-dihydro-15-keto; 5,6DH, 5,6-dihydro.

TABLE 6. Product ions detected by MS/MS after fragmentation of molecular anions [M-H]$^-$ of taurine conjugates of $PGF_{2\alpha}$, Class III F2-iPs and their metabolites

Modification of PGF_2 Structure	[M-H]$^-$	-H_2O	-C_2H_4O	-H_2O -C_2H_4O	-(C16-C20) -H	-H_2O -(C16–C20) +H	-C_2H_4O- hexanal	CH_2 $(CH)_2$ $(CH_2)_2$ CONH $(CH_2)_2$ SO_3^-	$(CH_2)_2$ CONH $(CH_2)_2$ SO_3^-	CH_2 CONH $(CH_2)_2$ SO_3^-	CONH $(CH_2)_2$ SO_3^-	NH $(CH_2)_2$ SO_3^-	$(CH_2)_2$ SO_3^-	SO_3^-
	m/z													
1-Tauro	460	442	416		388	372	316	233	178	165	151	124	107	80
1-Tauro-13,14DH-15K	460	442						233	178		151	124	107	80
1-Tauro-2,3-dinor	432		388	370							151	124		
1-Tauro-13,14DH-15K-2,3-dinor	432	414									151	124	107	80
1-Tauro-2,3-dinor-5,6-DH	434		390	372	362	346				165		124	107	80
1-Tauro-13,14DH-15K-2,3-dinorDH	434	416								165		124	107	80

1-Tauro, taurine conjugate at C1; 13,14DH-15K, 13,14-dihydro-15-keto; 5,6DH, 5,6-dihydro.

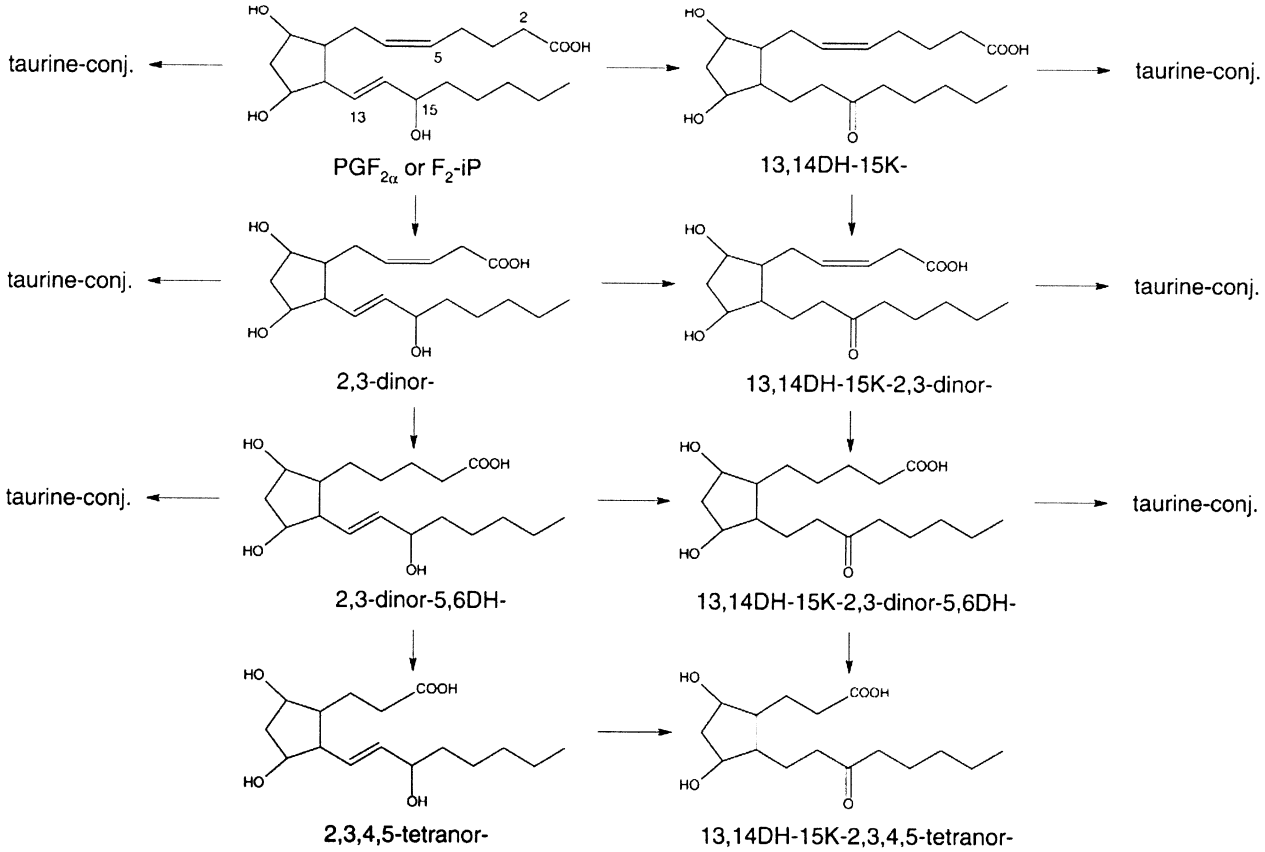

Fig. 7. Structures of unconjugated metabolites identified in this study. Formation of taurine conjugates at C1 (taurine-conj) is also indicated (structures shown in Fig. 8).

ing with $^{18}O_2$, indicating retention of the carboxyl (22). Our data indicate that for 2,3-dinor-5,6-dihydro-8-*epi*-$PGF_{2\alpha}$, this fragment is instead due to the loss of CO_2, and not C_2H_4O, in addition to part of the ω-chain.

2,3,4,5-TETRANOR METABOLITE. A metabolite with a 2,3,4,5-tetranor structure, resulting from two β-oxidation steps, was common to $PGF_{2\alpha}$ and all F_2-iPs (Table 1), indicating that this pathway [in addition to conjugation with taurine (see below)] is the least affected by the stereochemical structure of the parent compound. This was a prominent product for all diastereoisomers, except 15*S*-*ent*-8-*epi*-$PGF_{2\alpha}$, which had a much more abundant 13,14-dihydro-15-keto-2,3,4,5-tetranor metabolite (see below). Our previous characterization of the 2,3,4,5-tetranor metabolites of $PGF_{2\alpha}$ and 8-*epi*-$PGF_{2\alpha}$ (9) helped prove the identity of the other diastereoisomeric metabolites. The chromatographic and mass spectral characteristics of the nine diastereoisomeric 2,3,4,5-tetranor metabolites (Tables 2 and 3) clearly support their identity. The MS/MS spectra of the carboxylate anion (*m/z* 299) showed a fragmentation consistent with the proposed structure (Table 4 and Fig. 5). All ions conserving the α-chain were found, as expected, at a *m/z* value 54 amu less than the corresponding ions of the parent compound.

13,14-DIHYDRO-15-KETO METABOLITE. A metabolite with this structure was found for $PGF_{2\alpha}$ and for two of the F_2-iPs, namely 8-*epi*-$PGF_{2\alpha}$ and 15*S*-*ent*-8-*epi*-$PGF_{2\alpha}$ (Table 1). The product deriving from $PGF_{2\alpha}$ had GC-NICIMS and HPLC-MS/MS behavior identical to authentic 13,14-dihydro-15-keto-$PGF_{2\alpha}$ (Tables 2 and 3, and Fig. 4). On GC, the two syn/anti isomers due to derivatization of the keto group to methoxime eluted shortly after the parent compounds, as a single broad peak for 13,14-dihydro-15-keto-$PGF_{2\alpha}$ but as separate peaks for the metabolites from 8-*epi*-$PGF_{2\alpha}$ and 15*S*-*ent*-8-*epi*-$PGF_{2\alpha}$ (Table 2 and Fig. 2). On HPLC, the 13,14-dihydro-15-keto diastereoisomeric metabolites eluted about 3 min later than their parent compounds (Table 3 and Fig. 3). The MS/MS spectra of hepatocyte-derived and authentic 13,14-dihydro-15-keto-$PGF_{2\alpha}$ are shown in Fig. 4. On account of their identical molecular weight, the 13,14-dihydro-15-keto metabolite and the parent compound have the same mass-to-charge ratio for the carboxylate anion and several product ions (Table 4). The MS/MS spectrum of the 13,14-dihydro-15-keto metabolite can, however, be clearly distinguished by the prominent ions at *m/z* 113, 183, and 195, and the very low abundance of *m/z* 193 (base peak in the parent compound). The corresponding metabolites from 8-*epi*-$PGF_{2\alpha}$ and 15*S*-*ent*-8-*epi*-$PGF_{2\alpha}$ had identical MS/MS spectra (not shown).

13,14-DIHYDRO-15-KETO-2,3-DINOR METABOLITE. A compound with this structure was found only as a minor product of 8-*epi*-$PGF_{2\alpha}$ (Table 1). This metabolite was identified by observing its GC-NICIMS and HPLC-MS/MS characteristics, which are consistent with its putative structure. In

particular, GC-NICIMS analysis showed the peak doublet of the syn/anti isomers (RT = 10.7 and 10.8 min) at *m/z* 498 when derivatized to methoxime, but a single peak (RT = 10.9 min) at *m/z* 469 (29 amu less, corresponding to the different groups at C-15, i.e., $C{=}NOCH_3$ vs. C=O), when the keto group was not derivatized (not shown). The MS/MS spectrum, although poorly informative, was very similar to that of the corresponding metabolite without the 13,14-dihydro-15-keto modification (Table 4), except for a difference in the most abundant ion (base peak at *m/z* 263).

13,14-DIHYDRO-15-KETO-2,3-DINOR-5,6-DIHYDRO METABOLITE. A compound with this structure was found only as a minor product of $PGF_{2\alpha}$ and 8-*epi*-$PGF_{2\alpha}$ (Table 1). This metabolite was identified by direct comparison with authentic 13,14-dihydro-15-keto-2,3-dinor-5,6-dihydro-*ent*-8-*epi*-$PGF_{2\alpha}$ using both GC-NICIMS and HPLC-MS/MS (Tables 2 and 3). The MS/MS spectra of the standard and the metabolite from $PGF_{2\alpha}$ are shown in Fig. 6. The mass spectrum was similar for the corresponding metabolite derived from 8-*epi*-$PGF_{2\alpha}$ (not shown). As observed for the C20 analogs, although the MS/MS spectra of the 13,14-dihydro-15-keto-2,3-dinor-5,6-dihydro metabolite and its 2,3-dinor-5,6-dihydro analog have the same mass-to-charge ratio for the precursor (*m/z* 327) and some product ions, the former can be clearly distinguished by the prominent ion at *m/z* 113, typical of all metabolites bearing the 13,14-dihydro-15-keto modification, and the absence of an ion at *m/z* 111 (Fig. 6).

13,14-DIHYDRO-15-KETO-2,3,4,5-TETRANOR METABOLITE. A prominent product with this structure was found for $PGF_{2\alpha}$, and among F_2-iPs, for 8-*epi*-$PGF_{2\alpha}$, 15*S*-*ent*-8-*epi*-$PGF_{2\alpha}$, 12-*epi*-$PGF_{2\alpha}$, and *ent*-12-*epi*-$PGF_{2\alpha}$ (Table 1). For 15*S*-*ent*-8-*epi*-$PGF_{2\alpha}$, this was by far the most abundant metabolite. These compounds were identified by comparing their MS/MS spectra (Fig. 5) with two authentic C20 and C18 homologs, 13,14-dihydro-15-keto-$PGF_{2\alpha}$ and 13,14-dihydro-15-keto-2,3-dinor-5,6-dihydro-*ent*-8-*epi*-$PGF_{2\alpha}$ (Figs. 4 and 6). As expected, the 13,14-dihydro-15-keto-2,3,4,5-tetranor metabolite had the carboxylate anion (*m/z* 299) and most of the product ions at the same *m/z* value as the 2,3,4,5-tetranor metabolite, except for the expected major ion at *m/z* 113 (Fig. 5). HPLC and GC behavior, as well as the NICIMS features of all isomers, were consistent with this putative structure (Tables 2 and 3). The presence of the keto group was also confirmed, e.g., for 13,14-dihydro-15-keto-2,3,4,5-tetranor-8-*epi*-$PGF_{2\alpha}$, by observing that the two peaks (syn/anti isomers) eluting after 9.5 and 9.6 min at *m/z* 472 disappeared when the keto group was not derivatized to methoxime, whereas a peak appeared at *m/z* 443 after 9.7 min, as expected (not shown).

Taurine conjugates. Taurine conjugates of parent $PGF_{2\alpha}$, F_2-iPs, and their prominent C20 and C18 metabolites were identified on the basis of their HPLC behavior (**Table 5** and **Fig. 8**) and MS/MS spectra (**Table 6**, Fig. 8, and **Fig. 9**). Some of these spectra showed striking similarities with those described by Hankin et al. (20) for the cor-

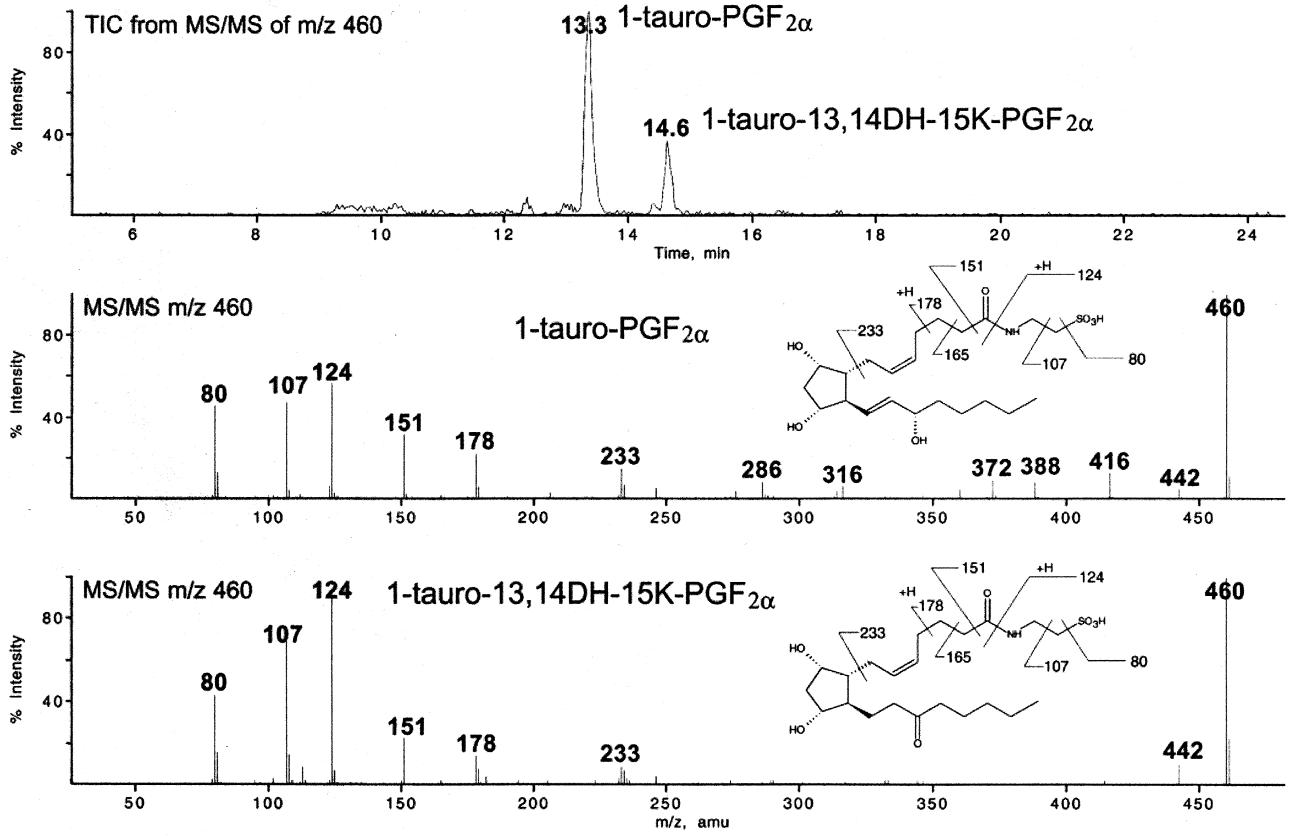

Fig. 8. HPLC-MS/MS tracing of TIC and MS/MS spectra obtained from collision-activated decomposition of the molecular anions (*m/z* 460; 56 eV) of hepatocyte-derived 1-tauro-$PGF_{2\alpha}$, and 1-tauro-13,14-dihydro-15-keto-$PGF_{2\alpha}$. HPLC retention time is indicated for each metabolite.

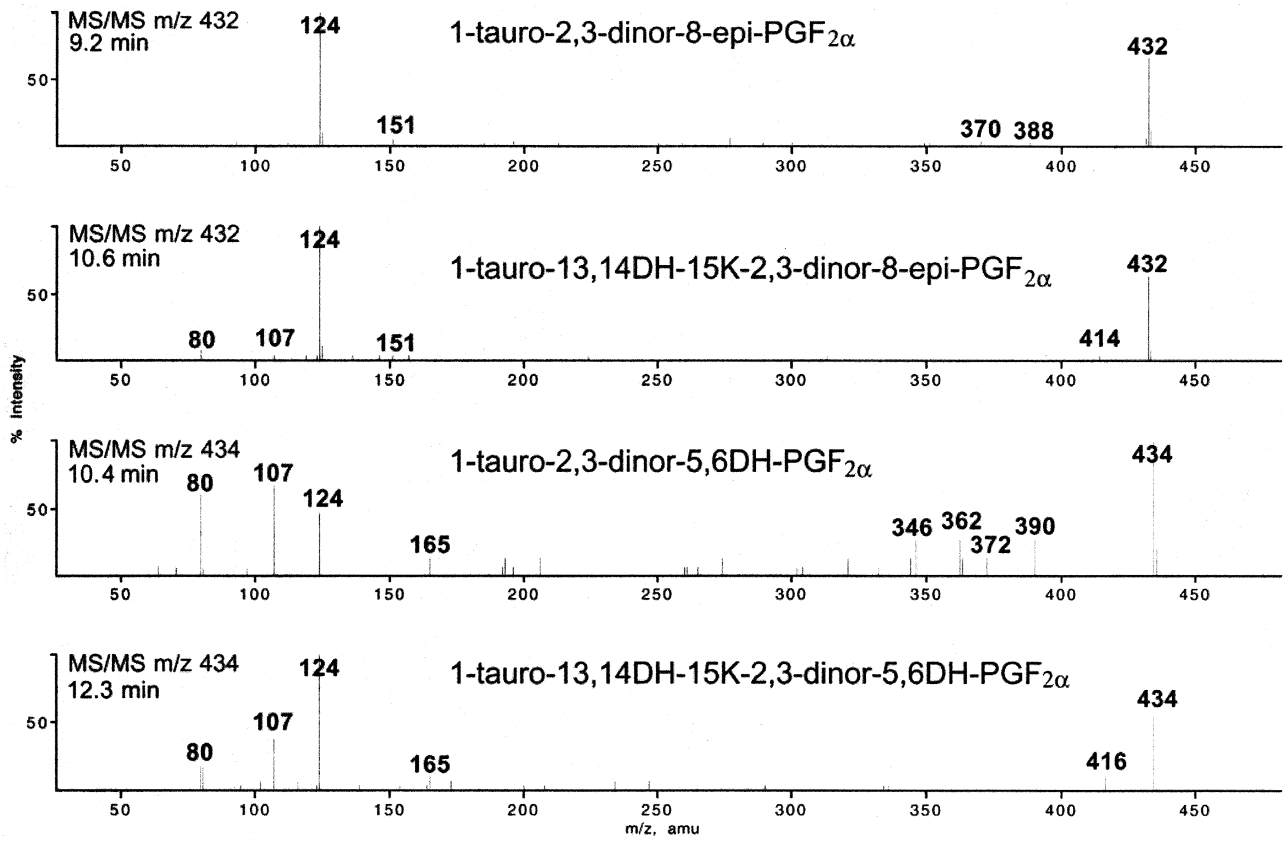

Fig. 9. MS/MS spectra obtained from collision-activated decomposition of the molecular anions of hepatocyte-derived 1-tauro-2,3-dinor-8-*epi*-$PGF_{2\alpha}$ and 1-tauro-13,14-dihydro-15-keto-2,3-dinor-8-*epi*-$PGF_{2\alpha}$ (*m/z* 432; 42 eV) plus 1-tauro-2,3-dinor-5,6-dihydro-$PGF_{2\alpha}$ and 1-tauro-13,14-dihydro-15-keto-2,3-dinor-5,6-dihydro-$PGF_{2\alpha}$ (*m/z* 434; 56 eV). HPLC retention time is indicated for each metabolite.

responding taurine conjugates of PGE_2 and its metabolites. Because no reference compounds were available, we were not able to quantify these metabolites. However, taking the intensity of the total ion current generated by each of these compounds on HPLC-MS/MS as an approximate indicator of its relative abundance, for each diastereoisomer the total amount of taurine conjugates and unconjugated products was of about the same order of magnitude. This is in accordance with Hankin's study (20), showing comparable overall amounts of radioactivity associated with taurine-conjugated or unconjugated metabolites of ^{3}H-PGE_2 formed by isolated rat hepatocytes.

Excluding the taurine conjugates of 2,3-dinor and 13,14-dihydro-15-keto-2,3-dinor metabolites which gave a peculiar fragmentation, like their unconjugated counterparts, the MS/MS spectra of taurine conjugates showed: *1*) prominent ions derived from detachment of the entire or fragmented taurine group (*m/z* 124, $H_2N\text{-}CH_2\text{-}CH_2\text{-}SO_3^-$; *m/z* 107, $CH_2 = CH\text{-}SO_3^-$; *m/z* 80, SO_3^-), or *2*) ions derived from retention of the charge on the PGF backbone with loss of H_2O and/or C_2H_4O (Table 6). Other prominent ions correspond to fragments of the α-chain conjugated with taurine (for the parent compounds, *m/z* 151, 178, and 233, corresponding to taurine attached to C1, C1–C3, and C1–C7). Of these, the smallest fragment at *m/z* 151 ($CONH(CH_2)_2SO_3^-$) was common to all C18 and C20 conjugates. As shown by Hankin et al. (20) for taurine conjugates of PGE_2 and its metabolites, these products tend to be scarcely fragmented under standard MS/MS conditions, except for the taurine-dinor metabolite, which shows easy detachment of the taurine group, but no other significant fragment except at *m/z* 124. High collision energy (56 eV) was therefore used to obtain structurally informative MS/MS spectra of the taurine conjugates, except for 1-tauro-2,3-dinor and 1-tauro-13,14-dihydro-15-keto-2,3-dinor metabolites (42 eV).

As observed for unconjugated metabolites, the 13,14-dihydro-15-keto modification does not alter the molecular weight, so that MS/MS spectra have the molecular anions and many fragment ions at the same *m/z* values. However, a common feature of the MS/MS spectra of all tauro-conjugates with the 13,14-dihydro-15-keto modification was the absence of prominent ions in the central part of the mass spectrum (Table 6, and Figs. 8 and 9).

TAURINE CONJUGATES OF C20 COMPOUNDS. A taurine conjugate of the parent compound was observed for $PGF_{2\alpha}$ and all F_2-iP diastereoisomers (Table 1). This was by far the most abundant of all conjugates for all diastereoisomers, except for 15*S-ent*-8-*epi*-$PGF_{2\alpha}$, which, instead, had a more prominent 1-tauro-13,14-dihydro-15-keto metabolite, in accordance with 15-OH dehydrogenation being a preferential pathway for this diastereoisomer. The least abundant

conjugate was found for 15*S*-*ent*-12-*epi*-$PGF_{2\alpha}$, in agreement with its scarce overall metabolism. In addition to the prominent 1-tauro-13,14-dihydro-15-keto metabolite of 15*S*-*ent*-8-*epi*-$PGF_{2\alpha}$, other 1-tauro-13,14-dihydro-15-keto-metabolites were found as minor products of the isomers forming the corresponding unconjugated metabolite, i.e., $PGF_{2\alpha}$ and 8-*epi*-$PGF_{2\alpha}$, (Table 1). This was taken in addition to the chromatographic and mass spectral behavior (Tables 5 and 6, and Fig. 8), as further proof of their identity in the absence of reference material.

TAURINE CONJUGATES OF C18 METABOLITES. Taurine conjugates were identified for all major diastereoisomeric C18 metabolites (Table 1). In particular, we identified: *1*) 1-tauro-2,3-dinor metabolites of 8-*epi*-$PGF_{2\alpha}$, 15*R*-8-*epi*-$PGF_{2\alpha}$, 12-*epi*-$PGF_{2\alpha}$, and *ent*-12-*epi*-$PGF_{2\alpha}$; *2*) 1-tauro-2,3-dinor-5,6-dihydro metabolites of $PGF_{2\alpha}$, 12-*epi*-$PGF_{2\alpha}$ and *ent*-12-*epi*-$PGF_{2\alpha}$; *3*) 1-tauro-13,14-dihydro-15-keto-2,3-dinor metabolites of 8-*epi*-$PGF_{2\alpha}$ (minor metabolite); and *4*) 1-tauro-13,14-dihydro-15-keto-2,3-dinor-5,6-dihydro metabolites of $PGF_{2\alpha}$. HPLC-MS/MS features of these metabolites are shown in Table 5, and representative MS/MS spectra are shown in Fig. 9 and interpreted in Table 6.

TAURINE CONJUGATES OF C16 METABOLITES. Although MS/MS spectra of sufficient intensity could not be recorded for taurine conjugates of C16 metabolites, preliminary evidence obtained by multiple reaction monitoring of the precursor-to-product ion transition from *m/z* 406 to *m/z* 124 suggests that very small amounts of these conjugates were present in the hepatocyte medium. The most prominent unconjugated C16 metabolites with and without the 13,14-dihydro-15-keto modification had their corresponding taurine conjugate as a small product (data not shown). Hankin et al. (20) also found that the taurine conjugate of tetranor-PGE_2 was a minor component of the metabolic profile.

Metabolic profiles of $PGF_{2\alpha}$ and F_2-iPs

In a first experiment to establish the best experimental conditions for the identification study, $PGF_{2\alpha}$ and 8-*epi*-$PGF_{2\alpha}$ were incubated separately for 10, 20, and 40 min. Quantitation by GC-NICIMS of unconjugated metabolites in the incubation medium and cell lysate indicated that: *1*) all unconjugated metabolites accumulated with time in the medium (sum of metabolites formed per plate: ~5–10 ng/min), while their abundance remained constant in time in the cell lysate; and *2*) the amount of the parent compounds decreased with time in the medium, reaching ~150 ng/ml at 40 min, but was low at any time in the hepatocyte lysate (<20 ng).

Other GC-NICIMS measurements showed that, after 20 min of incubation, the unmetabolized compound in the medium was reduced to 50–60% of the initial amount for $PGF_{2\alpha}$, 8-*epi*-$PGF_{2\alpha}$, and 12-*epi*-$PGF_{2\alpha}$, ~70% for 15*R*-8-*epi*-$PGF_{2\alpha}$, *ent*-12-*epi*-$PGF_{2\alpha}$, and 15*R*-12-*epi*-$PGF_{2\alpha}$, ~80% for *ent*-8-*epi*-$PGF_{2\alpha}$ and 15*S*-*ent*-8-*epi*-$PGF_{2\alpha}$, and 95% for 15*S*-*ent*-12-*epi*-$PGF_{2\alpha}$. This is in agreement with the abundance profile of total metabolites (unconjugated plus conjugated) from the various diastereoisomers ($PGF_{2\alpha} \cong$ 8-*epi*-$PGF_{2\alpha} \cong$ 12-*epi*-$PGF_{2\alpha} >$ 15*R*-8-*epi*-$PGF_{2\alpha} \cong$ *ent*-12-*epi*-$PGF_{2\alpha} \cong$ 15*R*-12-*epi*-$PGF_{2\alpha} \geqslant$ *ent*-8-*epi*-$PGF_{2\alpha} \cong$ 15*S*-*ent*-8-*epi*- $PGF_{2\alpha} \geqslant$ 15*S*-*ent*-12-*epi*- $PGF_{2\alpha}$).

DISCUSSION

F_2-isoprostanes, a family of 64 compounds isomeric to $PGF_{2\alpha}$, are products of free radical-mediated non-enzymatic peroxidation of arachidonic acid (1–3). These compounds can be used to evaluate local or systemic lipid peroxidation in vivo, since they are detected esterified to tissue and plasma lipids and in the free form in body fluids (2–5). Increased F_2-iP levels were found in several experimental and clinical conditions associated with free radical-mediated oxidant damage (2–5). Given that F_2-iPs are becoming increasingly popular as oxidative stress markers, it is important to expand our knowledge about their formation and fate in vivo. Identification of the major metabolites of the various F_2-iP isomers, with the development of specific assays, may help evaluate the in vivo formation of selected compounds. This is of particular interest for the Type III regioisomer family, since the only compounds with proven biological activity so far are these diastereoisomers of $PGF_{2\alpha}$.

Isolated hepatocytes represent a well-characterized, rather simple system to screen for potential pathways of hepatic metabolism of endogenous and exogenous compounds (23). This in vitro system has the advantage of employing freshly isolated cells, with their intact enzymatic machinery, that reproducibly yield enough material for mass spectrometry identification of metabolites after rather simple purification procedures. This technique has been successfully used in the field of eicosanoids and isoprostanes (9, 17, 20).

We compared the metabolic fate of $PGF_{2\alpha}$ versus Type III F_2-iPs. Among the 16 possible diastereoisomers of the Type III family, we considered only the eight *cis* ring-substituted diastereoisomers that are believed to be the most abundant (6). We identified several products resulting from a combination of β-oxidation, reduction of Δ^5 and/or Δ^{13} double bonds, or 15-OH oxidation, plus taurine conjugates of parent compounds and their prominent C20 and C18 metabolites.

This study showed slight-to-marked stereo- and enantioselectivity in the different enzymatic steps involved in the metabolic transformations of $PGF_{2\alpha}$ and Type III F_2-iPs. Some compounds were extensively metabolized to a variety of products, while others were poorly metabolized, with specific stereochemical configurations favoring or impeding selected reactions. For example, the steric configuration of the hydroxyl at C-15 must be *S*, as in the cyclooxygenase-derived PG, for 15-OH dehydrogenation to occur easily. In fact, no metabolites with the 15-keto modification (unconjugated or conjugated) were formed from diastereoisomers with the 15*R* configuration, except for the 13,14-dihydro-15-keto-2,3,4,5-tetranor metabolites of *ent*-8-*epi*-$PGF_{2\alpha}$ (minor product) and *ent*-12-*epi*-$PGF_{2\alpha}$. The Δ^{13} double bond of prostaglandin (PG) cannot be reduced without prior 15-OH dehydrogenation (17). This appears to be true for F_2-iPs too, as all metabolites with the

13,14-dihydro modification had the concomitant presence of the 15-keto group.

Another reaction that was markedly influenced by the steric structure was the reduction of Δ^5 double bond, which proceeded easily for $PGF_{2\alpha}$, but was more or less impeded for the various enantiomeric pairs of F_2-iPs. The pathways that were the least affected by the stereochemical configuration were β-oxidation and taurine conjugation, which gave rise to at least one product each, even for the scantly metabolized 15*S-ent*-12-*epi*-$PGF_{2\alpha}$.

The finding of significant amounts of taurine conjugates of $PGF_{2\alpha}$, F_2-iPs, and their prominent C20 and C18 metabolites drew our attention to the fact that, apart from the 13,14-dihydro-15-keto metabolites, all the other products identified here are formed through activation of the carboxyl group to a CoA-thioester. It is generally accepted that both β-oxidation and taurine conjugation of carboxylic acids occur after the formation of a reactive CoA thioester intermediate (24). For $PGF_{2\alpha}$ and F_2-iPs, this common precursor appears to be easily formed for C20 and C18 products, because there is subsequent formation of *1*) unconjugated C18 and C16 products through β-oxidation, and *2*) taurine conjugates of C20 and C18 products through taurine-*N*-acyltranferase activity. The fact that β-oxidation does not proceed further to C14 products and that the C16 metabolites, although abundant, are poorly conjugated with taurine, suggests, among other possibilities, a scant formation of the precursor CoA-thioester of the C16 metabolites. Due to the presence of this common activation step for most of the prominent metabolites of $PGF_{2\alpha}$ and F_2-iPs, xenobiotic carboxylic acids that are metabolized through the corresponding CoA-thioesters might cause inhibition and/or diversion of $PGF_{2\alpha}$ and F_2-iPs metabolism in vivo. An example of such drugs are the widely used 2-arylpropionic non-steroidal anti-inflammatory drugs (24). This should be taken into consideration when measurements of F2-iPs or their selected metabolites in body fluids are used for assessing their formation in vivo.

Although a detailed quantitative description of $PGF_{2\alpha}$ and F_2-iP metabolism by isolated rat hepatocytes was beyond the scope of this study, for each diastereoisomer the total amounts of conjugated and unconjugated products were in general of the same order of magnitude. Although this cannot be taken as proof that these products are of comparable abundance in vivo, it certainly shows that these cells have an efficient enzymatic machinery for both pathways, and that these metabolites may therefore be formed in vivo, at least in the rat.

Many in vivo studies in different mammalian species found that exogenous $PGF_{2\alpha}$ is metabolized through common enzymatic pathways, including those discussed above (14–16, 18, 19). Nevertheless, not only are the prominent circulating and urinary metabolites different in the various species, but even in the same species the mode of administration may alter the metabolic profile of $PGF_{2\alpha}$ (16, 18, 19). Searching for the major metabolites of the endogenously formed, rather than exogenously administered, compounds in each species would hence be the best approach, but this can be extremely difficult in the absence of any preliminary analytical characterization of potential in vivo metabolites. A simplified approach such as that described here, despite suffering from the obvious intrinsic limitations of an in vitro study, allows, in principle, the obtaining of useful information for subsequent in vivo studies aimed at identifying the main endogenous products.

If their presence is proved in vivo, some of the metabolites identified here might become useful targets of new assays for determining overall F2-iP formation, or for evaluating the in vivo formation and fate of a specific bioactive diastereoisomer. Selected metabolites might also be chosen for their particular steric configurations or their greater abundance in vivo, for developing immunoassays with minimal cross-reactivity against endogenous cyclooxygenase-derived metabolites.

In conclusion, we showed how the different Type III F_2-iP diastereoisomers are degraded through pathways of $PGF_{2\alpha}$ metabolism, with metabolic profiles depending on their steric configuration. These data, together with our structural and analytical characterization of the metabolites, may be useful as a basis for further investigating F_2-iP disposition in vivo.

Claudia Rivalta is a fellow of the Fondazione A. e A. Valenti.

Manuscript received 2 October 2001 and in revised form 19 November 2001.

REFERENCES

1. Morrow, J. D., K. E. Hill, R. F. Burk, T. M. Nammour, K. F. Badr, and L. J. Roberts, II. 1990. A series of prostaglandin F_2-like compounds are produced in vivo in humans by a non-cyclooxygenase, free radical-catalyzed mechanism. *Proc. Natl. Acad. Sci. USA.* **87:** 9383–9387.
2. Roberts, II, L. J., and J. D. Morrow. 2000. Measurement of F_2-isoprostanes as an index of oxidative stress in vivo. *Free Radical Biol. Med.* **28:** 505–513.
3. Lawson, J. A., J. Rokach, and G. A. FitzGerald. 1999. Isoprostanes: formation, analysis and use as indices of lipid peroxidation in vivo. *J. Biol. Chem.* **274:** 24441–24444.
4. Delanty, N., M. Reilly, D. Praticò, D. J. Fitzgerald, J. A. Lawson, and G. A. FitzGerald. 1996. 8-epi-$PGF_{2\alpha}$: specific analysis of an isoeicosanoid as an index of oxidant stress in vivo. *Br. J. Clin. Pharmacol.* **42:** 15–19.
5. Praticò, D. 1999. F_2-isoprostanes: sensitive and specific noninvasive indices of lipid peroxidation in vivo. *Atherosclerosis.* **147:** 1–10.
6. Rokach, J., S. P. Khanapure, S-W. Hwang, M. Adiyaman, J. A. Lawson, and G. A. FitzGerald. 1997. The isoprostanes: a perspective. *Prostaglandins.* **54:** 823–851.
7. Waugh, R. J., J. D. Morrow, L. J. Roberts, II, and R. C. Murphy. 1997. Identification and relative quantitation of F2-isoprostane regioisomers formed in vivo in the rat. *Free Radical Biol. Med.* **23:** 943–954.
8. Roberts II, L. J., K. P. Moore, W. E. Zackert, J. A. Oates, and J. D. Morrow. 1996. Identification of the major urinary metabolite of the F2-isoprostane 8-iso-prostaglandin $F_{2\alpha}$ in humans. *J. Biol. Chem.* **271:** 20617–20620.
9. Chiabrando, C., A. Valagussa, C. Rivalta, T. Durand, A. Guy, E. Zuccato, P. Villa, J-C. Rossi, and R. Fanelli. 1999. Identification and measurement of endogenous β-oxidation metabolites of 8-epi-prostaglandin $F_{2\alpha}$. *J. Biol. Chem.* **274:** 1313–1319.
10. Basu, S. 1998. Metabolism of 8-iso-prostaglandin $F_{2\alpha}$. *FEBS Letters.* **428:** 32–36.
11. Roland, A., T. Durand, T. Rondot, J-P. Vidal, and J-C. Rossi. 1996. A practical asymmetric synthesis of ent-12-epi-$PGF_{2\alpha}$ methyl ester. *Bull. Soc. Chim. Fr.* **133:** 1149–1154.

12. Guy, A., T. Durand, J-P. Vidal, and J-C. Rossi. 1997. Total synthesis of 15(RS)-5,6-dehydro-8-epi-PGF$_{2\alpha}$ methyl ester by a biomimetic process. *Tetrahedron Lett.* **38:** 1543–1546.
13. Durand, T., A. Guy, O. Henry, J-P. Vidal, J-C. Rossi, C. Rivalta, A. Valagussa, and C. Chiabrando. 2001. Total syntheses of four metabolites of 15-F$_{2t}$-isoprostane. *Eur. J. Org. Chem.* **4:** 809–819.
14. Granström, E., and B. Samuelsson. 1971. On the metabolism of prostaglandin F$_{2\alpha}$ in female subjects. *J. Biol. Chem.* **246:** 5254–5263.
15. Granström, E., and B. Samuelsson. 1971. On the metabolism of prostaglandin F$_{2\alpha}$ in female subjects. II. Structures of six metabolites. *J. Biol. Chem.* **246:** 7470–7485.
16. Green, K. 1971. The metabolism of prostaglandin F$_{2\alpha}$ in the rat. *Biochim. Biophys. Acta.* **231:** 419–444.
17. Sago, T., R. Nakayama, T. Okumura, and K. Saito. 1986. Metabolism of prostaglandins D2 and F$_{2\alpha}$ in primary cultures of rat hepatocytes. *Biochim. Biophys. Acta.* **879:** 330–338.
18. Sun, F. F. 1974. Metabolism of prostaglandin F$_{2\alpha}$ in the rat. *Biochim. Biophys. Acta.* **348:** 249–262.
19. Granström, E., H. Kindahl, and M. L. Swahn. 1982. Profiles of prostaglandin metabolites in the human circulation. Identification of late-appearing, long-lived products. *Biochim. Biophys. Acta.* **713:** 46–60.
20. Hankin, J. A., P. Wheelan, and R. C. Murphy. 1997. Identification of novel metabolites of prostaglandin E2 formed by isolated rat hepatocytes. *Arch. Biochem. Biophys.* **340:** 317–330.
21. Zirrolli, J. A., E. Davoli, L. Bettazzoli, M. Gross, and R. C. Murphy. 1990. Fast atom bombardment and collision-induced dissociation of prostaglandins and thromboxanes: some examples of charge remote fragmentation. *J. Am. Soc. Mass Spectrom.* **1:** 325–335.
22. Li, H., J. A. Lawson, M. Reilly, M. Adiyaman, S-W. Hwang, J. Rokach, and G. A. FitzGerald. 1999. Quantitative high performance liquid chromatography/tandem mass spectrometric analysis of the four classes of F$_2$-isoprostanes in human urine. *Proc. Natl. Acad. Sci. USA.* **96:** 13381–13386.
23. Berry, M. N., H. J. Halls, and M. B. Grivell. 1992. Techniques for pharmacological and toxicological studies with isolated hepatocyte suspensions. *Life Sci.* **51:** 1–16.
24. Hutt, A. J., and J. Caldwell. 1990. Amino acid conjugation. *In* Conjugation Reactions in Drug Metabolism. G. J. Mulder, editor. Taylor & Francis, London. 273–305.